

Pinning down top dipole moments with ultra-boosted tops

Juan A. Aguilar–Saavedra^(a), Benjamin Fuks^(b,c) and Michelangelo L. Mangano^(c)

^(a) *Departamento de Física Teórica y del Cosmos, Universidad de Granada, E-18071 Granada, Spain*

^(b) *Institut Pluridisciplinaire Hubert Curien/Département Recherches Subatomiques, Université de Strasbourg/CNRS-IN2P3, 23 Rue du Loess, F-67037 Strasbourg, France*

^(c) *CERN, PH-TH, CH-1211 Geneva 23, Switzerland*

We investigate existing and future hadron-collider constraints on the top dipole chromomagnetic and chromoelectric moments, two quantities that are expected to be modified in the presence of new physics. We focus first on recent measurements of the inclusive top pair production cross section at the Tevatron and at the Large Hadron Collider. We then analyse the role of top-antitop events produced at very large invariant masses, in the context of the forthcoming 13-14 TeV runs of the LHC, and at a future 100 TeV proton-proton collider. In this latter case, the selection of semileptonic decays to hard muons allows to tag top quarks boosted to the multi-TeV regime, strongly reducing the QCD backgrounds and leading to a significant improvement in the sensitivity to anomalous top couplings.

I. INTRODUCTION

The first run of the Large Hadron Collider (LHC) at CERN has successfully confirmed the Standard Model (SM) of particle physics with the discovery of a Higgs boson with SM-like properties [1, 2]. Although no sign of physics beyond the SM has yet been observed, new phenomena at energies not far from the electroweak scale are predicted in many theories of new physics. There is therefore a great expectation for the upcoming LHC runs at center-of-mass (CM) energies $\sqrt{s} = 13$ TeV and 14 TeV, and for experiments at future accelerator facilities running at larger CM energies and luminosities. Furthermore, even if new physics were not directly reachable at the LHC or future machines, it might still be indirectly probed through precision measurements of the properties of the SM particles. In this context, the top quark is believed to play an important role, due to the closeness of its mass to the electroweak scale. This has motivated an intense research program dedicated to the study of its properties at the LHC. Future colliders will moreover be able to exploit the increase in CM energy and luminosity to probe indirect effects of new physics at higher momentum transfers, increasing the sensitivity to heavy new physics.

The conceptual design studies of new accelerator complexes for future circular colliders (FCC) have recently started, at CERN [3] and at IHEP [4]. Their ultimate goal is the operation of a proton-proton (pp) collider designed to operate at $\sqrt{s} = 100$ TeV. This accelerator will allow the exploration of energy scales several times higher than at the LHC, and will also significantly increase the statistics of known particles. For example, one trillion top quarks should be available with an integrated luminosity of 10 ab^{-1} . This consequently opens the door to indirect searches of new physics in the top sector with an unprecedented sensitivity.

In this paper we explore some of the opportunities of

fered by such a huge statistics of top quarks, focusing on the sensitivity to anomalous couplings to the gluons. The leading indirect effects from new physics present at a heavy scale Λ can be parametrized by adding to the SM Lagrangian \mathcal{L}_{SM} a set of dimension-six operators O_x invariant under the SM gauge symmetry [5–7],

$$\mathcal{L} = \mathcal{L}_{\text{SM}} + \mathcal{L}_{\text{eff}} = \mathcal{L}_{\text{SM}} + \sum_x \frac{C_x}{\Lambda^2} O_x + \dots, \quad (1)$$

where the Wilson coefficients C_x depend on the type of new physics and how it couples to the SM particles. After the spontaneous breaking of the electroweak symmetry, these operators generate corrections to the SM couplings included in \mathcal{L}_{SM} , as well as interactions not present at the tree level, such as electric dipole moments and explicit magnetic dipole moments. The effects on the top dipole moments can be parametrized by adding an effective term to the top-gluon gauge coupling,

$$\mathcal{L}_{\text{tg}} = -g_s \bar{t} \gamma^\mu \frac{\lambda_a}{2} t G_\mu^a + \frac{g_s}{m_t} \bar{t} \sigma^{\mu\nu} (d_V + i d_A \gamma_5) \frac{\lambda_a}{2} t G_{\mu\nu}^a, \quad (2)$$

with $G_{\mu\nu}^a$ ($a = 1, \dots, 8$) being the gluon field strength tensor, g_s the strong coupling constant, m_t the top mass and λ_a the Gell-Mann matrices. The second term above contains both $gt\bar{t}$ and $ggt\bar{t}$ interactions that arise, in the conventions of Refs. [7, 8], from the dimension-six operator

$$O_{uG\phi}^{33} = (\bar{q}_{L3} \lambda_a \sigma^{\mu\nu} t_R) \tilde{\phi} G_{\mu\nu}^a, \quad (3)$$

where q_{L3} denotes the weak doublet of left-handed quark fields of third generation, t_R the right-handed top quark field and ϕ is a weak doublet of Higgs fields (we define here $\tilde{\phi} = i\tau_2 \phi^*$). After electroweak symmetry breaking, this operator yields the top dipole moments

$$d_V = \frac{\sqrt{2} v m_t}{g_s \Lambda^2} \text{Re} C_{uG\phi}^{33}, \quad d_A = \frac{\sqrt{2} v m_t}{g_s \Lambda^2} \text{Im} C_{uG\phi}^{33}, \quad (4)$$

where $v = 246$ GeV is the vacuum expectation value of the neutral component of ϕ . For weakly-interacting new physics at the TeV scale, $C_{uG\phi}^{33} \sim \mathcal{O}(1)$ so that one expects $d_{V,A} \sim 0.05$. This exceeds both the chromomagnetic dipole moment generated in the SM at the one-loop level $d_V = -0.007$ [9] and the associated negligible chromoelectric moment [10].

Direct limits on the top chromomagnetic and chromoelectric dipole moments can be derived from measurements of the $t\bar{t}$ inclusive cross section at the Tevatron and the LHC [11–13], and of several $t\bar{t}$ differential distributions [14–16]. Moreover, weaker bounds have been recently calculated [17] from a CMS measurement of the $t\bar{t}$ spin correlation in LHC data at 8 TeV [18], as this observable is also modified by the anomalous interactions of Eq. (2). The most stringent limits on d_V and d_A however arise nowadays from low- Q^2 probes, such as measurements of the neutron electric dipole moment, which constrain $|d_A| \leq 9.5 \times 10^{-4}$ at the 90% confidence level (CL) [16], and rare B -meson decays, which imply $-3.8 \times 10^{-3} \leq d_V \leq 1.2 \times 10^{-3}$ at the 95% CL [19].

At the LHC running at 14 TeV, and even more at 100 TeV, a significant amount of top-antitop pairs with a multi-TeV invariant mass will be produced, with contributions dominated by the gluon-gluon fusion channel. These kinematical configurations with very large momentum transfer allow to explore the structure of the ttg couplings at the shortest distances, and should then be particularly sensitive probes of the top dipole moments [20, 21]. After reviewing the constraints that can be obtained from the measurements of total production cross sections, in this paper we therefore focus on the study of very high mass top-antitop final states, where the top quarks are necessarily highly boosted. We consider a simple-minded approach to extract the top-antitop signal from the large QCD background, and verify that, at 100 TeV, this is sufficient to significantly push the sensitivity to both chromoelectric and chromomagnetic dipole moments.

II. TEVATRON AND LHC LIMITS

The combination of inclusive $t\bar{t}$ cross section measurements at the Tevatron and the LHC provides much stronger limits on the top dipole moments than the individual measurements. The complementarity of these two colliders is due to a very different functional dependence of the total cross section on d_V and d_A at the Tevatron ($p\bar{p}$ collisions at 1.96 TeV) and the LHC (pp collisions at 7, 8 TeV), owing to the dominance of $q\bar{q} \rightarrow t\bar{t}$ at the former collider and $gg \rightarrow t\bar{t}$ at the latter. Making use of the FEYNRULES package [22, 23] to import the Lagrangian of Eq. (2) into MADGRAPH5_aMC@NLO [24], we evaluate the $t\bar{t}$ total production cross section at the Tevatron and the LHC with 8 TeV, $\sigma_{t\bar{t}}^{(2)}$ and $\sigma_{t\bar{t}}^{(8)}$ respectively, including the leading-order contributions of the top dipole moments. Since the amplitudes contain at

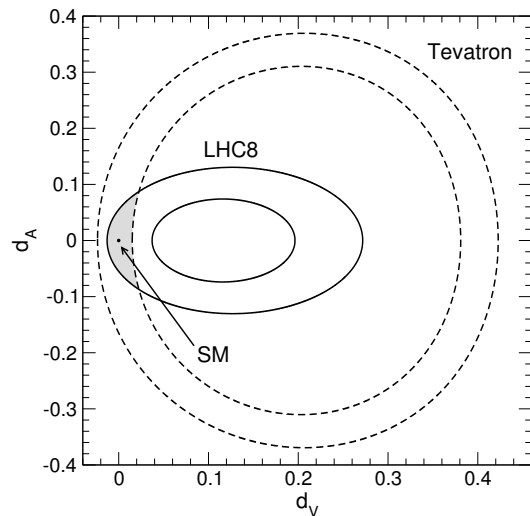


FIG. 1: Limits, at the 95% CL, on d_V and d_A as extracted from measurements of the top-pair production total cross section at the Tevatron (dashed) and the LHC with $\sqrt{s} = 8$ TeV (solid).

most two insertions of the anomalous vertices in Eq. (2), the dependence on d_A and d_V can be parametrized by a fourth-order polynomial in these two variables.¹ We find

$$\begin{aligned} \sigma_{t\bar{t}}^{(2)}(\text{pb}) &= \sigma_{\text{SM}}^{(2)}(\text{pb}) - 45.5 d_V + 131 d_V^2 - 64.7 d_V^3 \\ &\quad + 55.5 d_V^4 + 40.7 d_A^2 + 56.5 d_A^4 \\ &\quad - 66.2 d_V d_A^2 + 116 d_V^2 d_A^2, \\ \sigma_{t\bar{t}}^{(8)}(\text{nb}) &= \sigma_{\text{SM}}^{(8)}(\text{nb}) - 1.53 d_V + 10.1 d_V^2 - 23.0 d_V^3 \\ &\quad + 28.6 d_V^4 + 7.0 d_A^2 + 28.6 d_A^4 \\ &\quad - 23.1 d_V d_A^2 + 57.3 d_V^2 d_A^2, \end{aligned} \quad (5)$$

when employing the NNPDF 2.3 set of parton densities [25]. We extract the limits on d_V and d_A in Fig. 1 by using the most recent total rate measurements at the Tevatron, $\sigma_{\text{exp}}^{(2)} = 7.60 \pm 0.41$ pb [26], and the LHC with 8 TeV, $\sigma_{\text{exp}}^{(8)} = 241.5 \pm 8.5$ pb [27], together with the most precise SM predictions at the next-to-next-to-leading order accuracy in QCD, $\sigma_{\text{SM}}^{(2)} = 7.35 \pm 0.21$ pb and $\sigma_{\text{SM}}^{(8)} = 252.8 \pm 14.4$ pb [28]. In the results displayed

¹ We have made the choice of keeping all terms in the expansion of Eq. (5). Third-order and fourth-order terms do not play any role in the regions relevant for the combined limits. Quadratic terms correspond to contributions of order Λ^{-4} . Concerning the d_V^2 term, dimension-eight operators could generate additional contributions at the same Λ^{-4} order, and including them would change the interpretation of the limits obtained on d_V . On the other hand, dropping quadratic and higher-order terms, or equivalently truncating the series at order Λ^{-2} , would imply to neglect effects that formally appear at order Λ^{-4} but that are relevant in the extraction of the limits. We have therefore adopted the expansion of Eq. (5).

on Fig. 1, we define the SM case where there are no new physics contributions to the top dipole moments by $d_V = d_A = 0$. The shaded area corresponds to the overlap of the corresponding 95% CL allowed regions from the Tevatron (dashed) and the LHC (solid) measurements, and implies that $-0.012 \leq d_V \leq 0.023$ and $|d_A| \leq 0.087$. Our results are found compatible with the ones previously obtained in Ref. [13] and given at the 68.3% CL, and are stronger than the bounds derived from the spin correlation measurements [17, 18].²

With the important amount of $t\bar{t}$ data to be collected at the upcoming LHC run with pp collisions at 14 TeV, top dipole moments could be probed by going beyond the use of inclusive total cross sections, and could benefit from differential cross section measurements. For illustration, we consider three representative cases and focus on inclusive cross section measurements as well as on the production of $t\bar{t}$ pairs with an invariant mass $m_{t\bar{t}}$ required to be larger than either 1 TeV or 2 TeV. These last two observables are expected to exhibit an enhanced sensitivity to the top dipole moments because of the larger momentum transfers that are now (phase-space) favored and the specific Lorentz structure of the top dipole operators in Eq. (2). For the inclusive measurement, our predictions rely on standard $t\bar{t}$ reconstruction techniques so that the $t\bar{t}$ signal is considered well separable from the background, in a way similar to what has been achieved with collision data at 7 TeV and 8 TeV. We subsequently assume an overall uncertainty of 5% on the would-be measurement at 14 TeV. (For comparison, the 8 TeV measurement has a 3.5% uncertainty.)

When the $t\bar{t}$ system has an invariant mass $m_{t\bar{t}} > 1$ TeV or 2 TeV, the produced top quarks are usually boosted. This renders any associated measurement more difficult because of both the smaller statistics and the large QCD multijet contribution where a pair of boosted top and antitop quarks is faked. In order to realistically estimate the uncertainty that would be associated with measurements in such regimes, we restrict our analysis to $t\bar{t}$ pairs produced in the central region of the detector (with a pseudorapidity satisfying $|\eta| < 2$). This ensures a better performance of the top tagging algorithms due to a finer detector granularity, so that one could aim for a better rejection of the QCD background. We employ, in the $m_{t\bar{t}} > 1$ TeV (2 TeV) case, the third working point of CMS for top quarks with a transverse momentum $p_T > 400$ GeV (800 GeV) [30], so that a boosted top quark will be correctly tagged with an efficiency of about 12.5%, for a mistagging rate of a QCD jet as a top quark of about 0.03% (the studies of top-tagging performance by ATLAS are documented in Ref. [31]). We present, in

Invariant mass selection	$\sigma_{t\bar{t}}$	σ_{jj}	$\sqrt{S+B}/S$
$m_{t\bar{t}}$ (or m_{jj}) > 1 TeV	1.0 pb	0.89 pb	0.004
$m_{t\bar{t}}$ (or m_{jj}) > 2 TeV	16 fb	40 fb	0.047

TABLE I: Fiducial cross sections for boosted $t\bar{t}$ and dijet production at the LHC ($\sqrt{s} = 14$ TeV), after accounting for a centrality requirement and appropriate top tagging and misidentification rates. The sensitivities are normalized to 100 fb^{-1} of simulated collisions.

Table I, the corresponding fiducial cross sections for both the top-antitop signal and the multijet background, together with the sensitivity defined as $\sqrt{S+B}/S$ where S and B are the numbers of signal and background events normalized to a luminosity of 100 fb^{-1} , respectively.

We use the above results to deduce the statistical uncertainties that would be related to a fiducial cross section measurement in the large $m_{t\bar{t}}$ region for pp collisions at 14 TeV. Adding in quadrature systematic uncertainties, assumed to be 5%,³ we show, in Fig. 2, the limits expected to be extracted by using inclusive cross sections (solid black) and after imposing that the top-antitop systems under consideration have an invariant-mass larger than 1 TeV (solid blue annulus) and 2 TeV (solid red ellipse). For comparison, we superimpose the limits derived from inclusive cross section measurements at the Tevatron (dashed) while the bounds derived from the first LHC run, already presented in Fig. 1, are omitted as they are superseded by the potential LHC result at 14 TeV. Aside from the fact that limits derived when $m_{t\bar{t}}$ is required to be large are more constraining, the shape of the allowed region in the (d_V, d_A) plane changes for $m_{t\bar{t}} > 2$ TeV, turning out to be an ellipse instead of an annulus. This can be traced back to the smaller importance of the cubic terms d_V^3 , $d_V d_A^2$ in the expansion of the cross sections. For example, for $m_{t\bar{t}} > 2$ TeV,

$$\begin{aligned} \sigma_{t\bar{t}}^{(14)}(\text{pb}) = & \sigma_{\text{SM}}^{(14)}(\text{pb}) - 1.43 d_V + 75.1 d_V^2 - 226 d_V^3 \\ & + 4410 d_V^4 + 72.4 d_A^2 + 4410 d_A^4 - 229 d_V d_A^2 \\ & + 8830 d_V^2 d_A^2. \end{aligned} \quad (6)$$

Furthermore, despite the large coefficients, the quartic terms d_V^4 , d_A^4 and $d_V^2 d_A^2$ are always subleading for $d_{V,A} \lesssim 0.03$.

We estimate, with the shaded area in the figure, the 95% CL bounds derived from combining the inclusive and high- $m_{t\bar{t}}$ measurements at the LHC run II. The top dipole moments are constrained to fulfill

² After the completion of this work, an NLO calculation of the effects of a top chromo-magnetic moment has appeared [29]. Despite the different setup used in the computation, the resulting limits on d_V are rather similar to ours, and stable with respect to QCD corrections.

³ While this figure may seem optimistic for the high- $m_{t\bar{t}}$ tail measurement, one should also bear in mind that a simple counting experiment such as the cross section measurement above a given $m_{t\bar{t}}$ cut may be improved by a differential measurement. In this case, the high- $m_{t\bar{t}}$ tail is much more sensitive to top dipole moments than the region near threshold, which can be used for the reduction of the overall normalisation uncertainty.

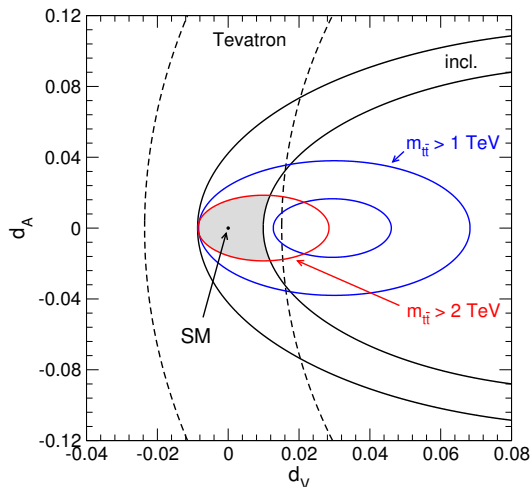


FIG. 2: Expected 95% CL limits on d_V and d_A at the future LHC run, with $\sqrt{s} = 14$ TeV. We show results using inclusive $t\bar{t}$ cross sections (solid black) and after considering only top-antitop pairs with an invariant mass larger than 1 TeV (solid blue annulus) and 2 TeV (solid red ellipse). For comparison, the Tevatron limit is also displayed (dashed).

$-0.0086 \leq d_V \leq 0.012$ and $|d_A| \leq 0.019$, so that the future run of the LHC is expected to improve the limits on d_V by a factor of two. Moreover, the sensitivity to a CP -violating chromoelectric moment using a CP -even observable — such as the $t\bar{t}$ fiducial cross section at high $m_{t\bar{t}}$ — is found remarkably similar to the expected one when measuring CP -odd triple product asymmetries ($|d_A| \leq 0.02$ [17]). Finally, assuming the Wilson coefficient $C_{uG\phi}^{33}$ to be of at most 4π , one can translate the bounds on d_V and d_A into a lower limit on the new physics scale Λ that is found to be $\Lambda \gtrsim 5$ TeV. (This ensures the validity of the effective field theory approach used in Eq. (2).) For smaller $C_{uG\phi}^{33}$ the limits on Λ are correspondingly looser.

III. SENSITIVITY AT 100 TEV

A significantly large number of $t\bar{t}$ pairs with a multi-TeV invariant mass are expected to be produced in several ab^{-1} of pp collisions at 100 TeV. With the opening of new kinematical regimes that have never been probed so far, the performance of the standard boosted top reconstruction techniques, developed in the LHC context and relying on the top-jet substructure [21, 30–41], needs to be reassessed, also in view of the potential improvements in the features of future detectors. Considering that a top quark with $p_T = 5$ TeV would have its three primary decay products contained within a cone of $R \lesssim 0.05$, it is clear that the effectiveness of a tagging based on the jet substructure would be strongly tied to the details of the detectors, such as tracking performance and calorimetric

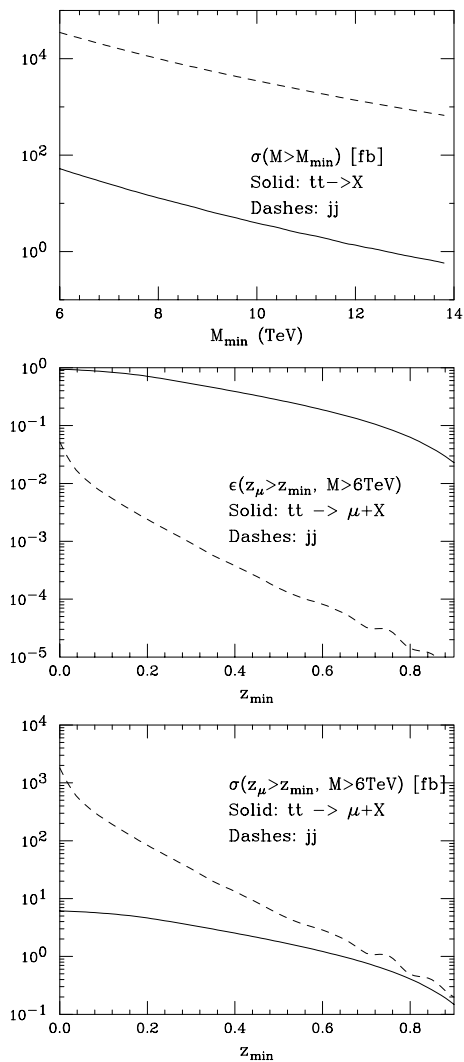


FIG. 3: Top: cross sections for inclusive $t\bar{t}$ and dijet final states, with the mass of the two leading jets above M_{min} (jets as defined in the text). Central: efficiency of the cut $z_\mu > z_{min}$, for $t\bar{t} \rightarrow \mu + X$ and for dijet events, with $M_{min} > 6$ TeV. Bottom: z_{min} dependence of the total rates for $t\bar{t} \rightarrow \mu + X$ and dijets, with $M_{min} > 6$ TeV.

granularity⁴. We therefore focus our study on a rather safe feature, in principle usable with any conceivable detector design, which should enable the differentiation of highly boosted top quarks from generic QCD jets. That is the spectrum of muons coming from the top decays, already discussed in the context of top tagging in Refs. [43–

⁴ After completion of this work, a study appeared [42], focused on the issue of tagging multi-TeV top jets. This paper confirms the potential for good tagging efficiency and background rejection, provided the detector performance can match the challenge of dealing with these high-density track environments.

45]. We show here that the study of this observable provides a proof of principle that a large-invariant-mass $t\bar{t}$ signal can be isolated from the otherwise overwhelming QCD background, in spite of the limited efficiency due to the branching ratio for a muonic decay. It is likely that more efficient top taggers, along the lines of what developed for the TeV regime of relevance to the LHC will significantly improve the usable statistics and our final sensitivity to anomalous top dipole moments.

We generate hard top-pair and dijet events with MADGRAPH5_aMC@NLO and further match them to the parton showering and hadronization algorithms included in the PYTHIA 8 program [46]. We then consider all central ($|\eta| < 2$) jets with $p_T > 1$ TeV reconstructed by making use of an anti- k_T algorithm with a radius parameter $R = 0.2$ [47], as implemented in the FASTJET package [48]. We finally analyse the reconstructed events with the MADANALYSIS 5 framework [49]. We preselect events featuring at least two reconstructed jets, and the invariant mass of the system made of the two leading jets (generically denoted by $m_{t\bar{t}}$) is demanded to be greater than some threshold M_{min} . In Fig. 3 (upper plot) we show the cross section as a function of the minimum dijet invariant mass M_{min} , both for the top signal and for the inclusive multijet background, which is over two orders of magnitude larger. As indicated above, in order to extract a top-antitop signal from the multijet QCD background, we further require at least one muon lying within a cone of $R = 0.2$ around any of the selected jets. This final step of the selection relies on the different properties of the muons arising from multijet and $t\bar{t}$ events. In the former case, they are found to only carry a small fraction of the jet transverse momentum, as inferred by their production from B -meson and D -meson decays, whereas in the latter case they are induced by prompt top decays and can get a significant fraction of the top transverse momentum. Events are consequently selected by requesting a minimum value z_{min} for the variable z_μ , defined by

$$z_\mu = \max_{i=1,\dots,n} \frac{p_T(\mu_i)}{p_T(j_i)}, \quad (7)$$

where we maximize, over the n muons possibly present in a given event, the ratio of the muon transverse momentum $p_T(\mu_i)$ to the corresponding jet transverse momentum $p_T(j_i)$. The efficiency of signal and background, as a function of the requirement on z_μ , are shown in the central plot of Fig. 3. In the case of the top signal, we removed from the definition of this efficiency the trivial branching ratio factor for the decay $t\bar{t} \rightarrow \mu + X$ (the contribution from muonic decays of the b hadrons is negligible in the relevant regions of z_μ). Since the z_μ distribution has a slight dependence on the transverse momentum of the jets, we show, as an example, the result averaged over the set of events with dijet invariant mass larger than 6 TeV. Convoluting the efficiencies with the appropriate rates, results in the cross sections shown in the bottom plot of Fig. 3. As we can see, imposing $z_\mu \gtrsim 0.5$ reduces the background by orders of magnitude,

Invariant mass selection	z selection	S/B	\mathcal{L}
$m_{t\bar{t}} > 6$ TeV	$z_\mu > 0.5$	0.39	36 fb $^{-1}$
$m_{t\bar{t}} > 10$ TeV	$z_\mu > 0.5$	0.74	200 fb $^{-1}$
$m_{t\bar{t}} > 15$ TeV	$z_\mu > 0.4$	0.25	2.4 ab $^{-1}$

TABLE II: Values of the selection threshold on the z_μ -variable of Eq. (7) for different invariant mass selections. We also present the related S/B ratio and the luminosity \mathcal{L} necessary for a 5σ extraction of a high- $m_{t\bar{t}}$ signal from the multijet background.

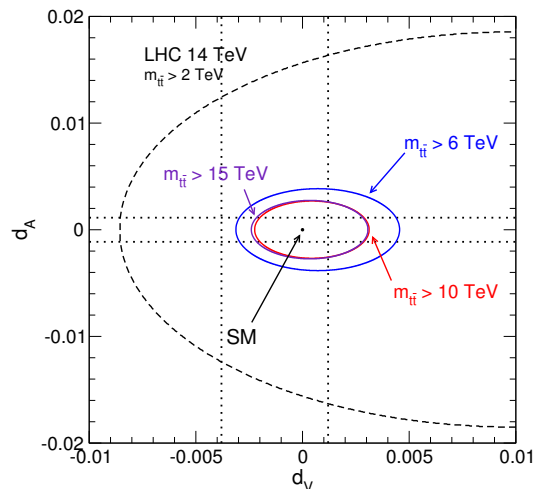


FIG. 4: Expected 95% CL limits on d_V and d_A at 100 TeV after considering top-antitop pairs with an invariant mass larger than 6 TeV (solid blue), 10 TeV (solid red) and 15 TeV (solid purple). For comparison, the expected limit from the second run of the LHC, with $m_{t\bar{t}} > 2$ TeV, (dashed line) and indirect limits (dotted lines) are also displayed.

down to a level comparable to the signal. Of course the experimental implementation of a selection like this will require a good muon identification efficiency in the dense jet environment, and a good momentum resolution in the multi-TeV momentum range. The study of the dijet rate, in the region of z_{min} where the background dominates, will provide nevertheless a good control sample for a robust data-driven determination of the absolute background normalization.

To generate the following results, we considered the three reference M_{min} thresholds of 6, 10 and 15 TeV. The corresponding requirements on the z_μ -variable, which we used to optimize the signal significance, are given in Table II. We also include here the luminosities that are necessary for a signal extraction at the 5σ level. We have verified that the results are similar when using HERWIG++ [50] instead of PYTHIA, or ALPGEN+HERWIG6 [51, 52].

Using the above results to deduce the statistical uncertainties associated with a would-be $t\bar{t}$ cross section measurement at 100 TeV, we additionally account for

systematic uncertainties of 5% before deriving the expectation for constraining the top dipole moments. (As previously discussed, we use a 5% systematic uncertainty as a reasonable reference value.) Assuming an integrated luminosity of 10 ab^{-1} , we display our results on Fig. 4, together with the limits expected from the LHC run at 14 TeV when using $t\bar{t}$ pairs with $m_{t\bar{t}} > 2 \text{ TeV}$. As for the LHC case, the selection on the top-antitop invariant mass enforces the contributions to the $t\bar{t}$ cross section that are quadratic in d_V and d_A to dominate, so that the allowed regions of the (d_V, d_A) plane are ellipses. As also suggested by Table II, the statistical uncertainties start to be important for large $m_{t\bar{t}}$ thresholds, so that the bounds derived when $m_{t\bar{t}} > 15 \text{ TeV}$ are similar to those obtained when $m_{t\bar{t}} > 10 \text{ TeV}$. An optimal $m_{t\bar{t}}$ selection would however strongly depend on the boosted top identification efficiency and mistagging rate, and may be different from the ones deduced in our simplified approach that only aims to show that the observation of $t\bar{t}$ pairs at high invariant mass can be envisaged. Enforcing $m_{t\bar{t}} > 10 \text{ TeV}$, the top dipole moments are bound to $-0.0022 \leq d_V \leq 0.0031$ and $|d_A| \leq 0.0026$, which improves the LHC results by about one order of magnitude, leading to constraints that are comparable to the indirect ones obtained from B -decays and from the neutron electric dipole moment. (In any case, direct and indirect limits are complementary, since the latter are much more model-dependent and can be evaded with additional new physics contributions.) Conversely, these limits can be translated in terms of a lower bound on the scale at which new physics could be expected, which is found to satisfy $\Lambda \gtrsim 17 \text{ TeV}$. This again ensures that the effective Lagrangian of Eq. (2) is valid with respect to the magnitude of the probed momentum transfers.

IV. SUMMARY

Direct limits on the top dipole couplings improve greatly by probing higher momentum transfers, as a consequence of their Lorentz structure. A 100 TeV pp collider is therefore a suitable machine to explore these anomalous interactions, in order to expose the indirect effects of new heavy states. In this paper, we have investigated the sensitivity of the future run of the LHC at 14 TeV and of a 100 TeV collider to anomalous top chromoelectric and chromomagnetic dipole moments d_V and d_A . We have considered both the study of $t\bar{t}$ inclusive cross sections and of top-antitop pairs with a multi-TeV invariant mass. The summary of our results is shown in Fig. 5 where we compare the current direct bounds to the projected limits for 100 fb^{-1} at 14 TeV and 10 ab^{-1} at 100 TeV.

The sensitivity at 100 TeV is expected to allow for a very important improvement of the bounds derived from measurements at the Tevatron and at the previous and future LHC runs, so that the d_V and d_A allowed ranges could be reduced by more than one order of magnitude

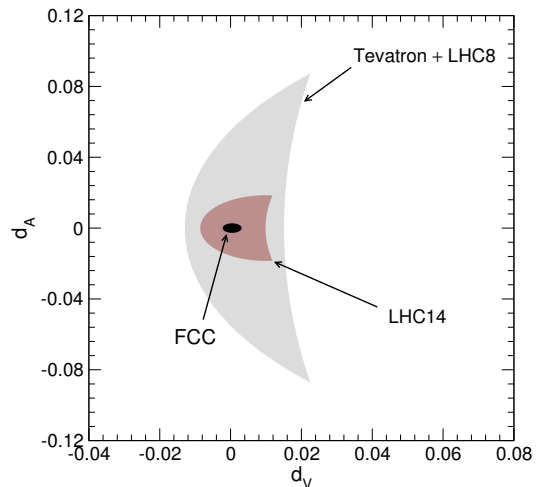


FIG. 5: Comparison of current and expected limits on the top dipole moments at the LHC and at 100 TeV.

with respect to the current direct limits. Furthermore, one may also wonder whether the expected LHC limits on d_V and d_A , obtained from $t\bar{t}$ spin correlation measurements and CP -odd triple product asymmetries, respectively, could be improved at 100 TeV (at the LHC, they are of the same order as the expected ones from cross section measurements in Fig. 2). Clearly, considering large energy scales — by selecting, for instance, high- $m_{t\bar{t}}$ top-antitop pairs as done in this work — enhances the effect on the anomalous contributions, not only in the fiducial cross section but also in the angular distributions. However, the angular distributions that may be measured in a typical LHC boosted top kinematical regime of $m_{t\bar{t}} \lesssim 2 \text{ TeV}$ (see, *e.g.*, Ref. [53]) may not be useful for ultra-boosted tops, and deserve further investigations. Further studies would also be desirable to evaluate the complementarity of the measurements discussed in this paper, with those possible with e^+e^- collisions at the top-antitop threshold, where a large statistics is foreseen by the e^+e^- option of the FCC complex [54], and at higher energies (*e.g.*, at CLIC [55] or ILC [56]).

As a byproduct of our study, we developed and described a new robust and effective approach to the problem of tagging top-antitop final states of large invariant mass, exploiting the hard muon spectrum in top decays. We are confident that more detailed studies of top-tagging algorithms, made possible also by the more aggressive detector technologies envisaged for the future collider experiments, can further improve our results.

What we showed is just an example of possible opportunities offered by the huge samples of top quarks available at a 100 TeV pp collider. Other areas that would certainly benefit include the study of rare or forbidden decays (*e.g.* $t \rightarrow q + g/Z/\gamma/H$ ($q = u, c$), tests of electroweak couplings (*e.g.* in s -channel single top production $pp \rightarrow W^* \rightarrow t\bar{b}$ at very large invariant mass), and high-precision measurements of production asymmetries,

spin correlations, etc. We look forward to future studies addressing these observables.

Acknowledgments

This work was supported by the ERC grant 291377, “LHCtheory: Theoretical predictions and analyses of

LHC physics: advancing the precision frontier”, by MICINN project FPA2010-17915 and MINECO project FPA2013-47836-C3-2-P, by FCT project EXPL/FIS-NUC/0460/2013, by the Junta de Andalucía projects FQM 101 and FQM 6552, and by the Théorie-LHC France initiative of the CNRS/IN2P3.

-
- [1] G. Aad *et al.* [ATLAS Collaboration], Phys. Lett. B **716** (2012) 1.
- [2] S. Chatrchyan *et al.* [CMS Collaboration], Phys. Lett. B **716** (2012) 30.
- [3] <http://cern.ch/fcc>.
- [4] <http://cepc.ihep.ac.cn>.
- [5] C. J. C. Burges and H. J. Schnitzer, Nucl. Phys. B **228** (1983) 464.
- [6] C. N. Leung, S. T. Love and S. Rao, Z. Phys. C **31** (1986) 433.
- [7] W. Buchmuller and D. Wyler, Nucl. Phys. B **268** (1986) 621.
- [8] J. A. Aguilar-Saavedra, Nucl. Phys. B **812** (2009) 181.
- [9] R. Martinez, M. A. Perez and N. Poveda, Eur. Phys. J. C **53** (2008) 221.
- [10] A. Soni and R. M. Xu, Phys. Rev. Lett. **69** (1992) 33.
- [11] P. Haberl, O. Nachtmann and A. Wilch, Phys. Rev. D **53** (1996) 4875.
- [12] Z. Hioki and K. Ohkuma, Eur. Phys. J. C **65** (2010) 127; Eur. Phys. J. C **71** (2011) 1535.
- [13] Z. Hioki and K. Ohkuma, Phys. Rev. D **88** (2013) 1, 017503.
- [14] K. m. Cheung, Phys. Rev. D **53** (1996) 3604.
- [15] Z. Hioki and K. Ohkuma, Phys. Rev. D **83** (2011) 114045.
- [16] J. F. Kamenik, M. Papucci and A. Weiler, Phys. Rev. D **85** (2012) 071501.
- [17] W. Bernreuther and Z. G. Si, Phys. Lett. B **725** (2013) 1-3, 115.
- [18] CMS Collaboration, CMS-PAS-TOP-14-005.
- [19] R. Martinez and J. A. Rodriguez, Phys. Rev. D **65** (2002) 057301.
- [20] C. Englert, A. Freitas, M. Spira and P. M. Zerwas, Phys. Lett. B **721** (2013) 261.
- [21] C. Englert, D. Goncalves and M. Spannowsky, Phys. Rev. D **89** (2014) 7, 074038.
- [22] A. Alloul, N. D. Christensen, C. Degrande, C. Duhr and B. Fuks, Comput. Phys. Commun. **185** (2014) 2250.
- [23] C. Degrande, C. Duhr, B. Fuks, D. Grellscheid, O. Mattelaer and T. Reiter, Comput. Phys. Commun. **183** (2012) 1201.
- [24] J. Alwall, R. Frederix, S. Frixione, V. Hirschi, F. Maltoni, O. Mattelaer, H.-S. Shao and T. Stelzer *et al.*, JHEP **1407** (2014) 079.
- [25] R. D. Ball, V. Bertone, S. Carrazza, C. S. Deans, L. Del Debbio, S. Forte, A. Guffanti and N. P. Hartland *et al.*, Nucl. Phys. B **867** (2013) 244.
- [26] T. A. Aaltonen *et al.* [CDF and D0 Collaborations], Phys. Rev. D **89** (2014) 072001.
- [27] ATLAS Collaboration, ATLAS-CONF-2014-054; CMS Collaboration, CMS-PAS-TOP-14-016.
- [28] M. Czakon, P. Fiedler and A. Mitov, Phys. Rev. Lett. **110** (2013) 252004.
- [29] D. B. Franzosi and C. Zhang, arXiv:1503.08841 [hep-ph].
- [30] CMS Collaboration, CMS-PAS-JME-13-007.
- [31] The ATLAS Collaboration, ATLAS-CONF-2013-084, ATLAS-COM-CONF-2013-074.
- [32] J. Thaler and L. T. Wang, JHEP **0807** (2008) 092.
- [33] D. E. Kaplan, K. Rehermann, M. D. Schwartz and B. Tweedie, Phys. Rev. Lett. **101** (2008) 142001.
- [34] L. G. Almeida, S. J. Lee, G. Perez, I. Sung and J. Virzi, Phys. Rev. D **79** (2009) 074012.
- [35] T. Plehn, G. P. Salam and M. Spannowsky, Phys. Rev. Lett. **104** (2010) 111801.
- [36] J. Thaler and K. Van Tilburg, JHEP **1202** (2012) 093.
- [37] T. Plehn, M. Spannowsky and M. Takeuchi, Phys. Rev. D **85** (2012) 034029.
- [38] D. E. Soper and M. Spannowsky, Phys. Rev. D **87** (2013) 5, 054012.
- [39] S. Schaetzel and M. Spannowsky, Phys. Rev. D **89** (2014) 014007.
- [40] M. Backovic, O. Gabizon, J. Juknevich, G. Perez and Y. Soreq, JHEP **1404** (2014) 176.
- [41] A. J. Larkoski, I. Moutl and D. Neill, arXiv:1411.0665 [hep-ph].
- [42] A. J. Larkoski, F. Maltoni and M. Selvaggi, arXiv:1503.03347 [hep-ph].
- [43] K. Rehermann and B. Tweedie, JHEP **1103** (2011) 059.
- [44] C. Brust, P. Maksimovic, A. Sady, P. Saraswat, M. T. Walters and Y. Xin, arXiv:1410.0362 [hep-ph].
- [45] B. Auerbach, S. Chekanov, J. Love, J. Proudfoot and A. V. Kotwal, arXiv:1412.5951 [hep-ph].
- [46] T. Sjostrand, S. Mrenna and P. Z. Skands, Comput. Phys. Commun. **178** (2008) 852.
- [47] M. Cacciari, G. P. Salam and G. Soyez, JHEP **0804** (2008) 063.
- [48] M. Cacciari, G. P. Salam and G. Soyez, Eur. Phys. J. C **72** (2012) 1896.
- [49] E. Conte, B. Fuks and G. Serret, Comput. Phys. Commun. **184** (2013) 222.
- [50] M. Bahr, S. Gieseke, M. A. Gigg, D. Grellscheid, K. Hamilton, O. Latunde-Dada, S. Platzer and P. Richardson *et al.*, Eur. Phys. J. C **58** (2008) 639.
- [51] M. L. Mangano, M. Moretti, F. Piccinini, R. Pittau and A. D. Polosa, JHEP **0307** (2003) 001.
- [52] G. Corcella, I. G. Knowles, G. Marchesini, S. Moretti, K. Odagiri, P. Richardson, M. H. Seymour and B. R. Webber, JHEP **0101** (2001) 010.
- [53] M. Baumgart and B. Tweedie, JHEP **1109** (2011) 049.
- [54] M. Bicer *et al.* [TLEP Design Study Working Group Collaboration], JHEP **1401** (2014) 164.
- [55] L. Linssen, A. Miyamoto, M. Stanitzki and H. Weerts, arXiv:1202.5940 [physics.ins-det].

- [56] G. Aarons *et al.* [ILC Collaboration], arXiv:0709.1893 [hep-ph].